Studies on highly active coordination catalysts for polymerization of α-olefins: 1. X-ray diffractomeric investigations of the catalyst supports

B. Keszler, G. Bodor and A. Simon
Research Institute for the Plastics Industry, Budapest, Hungary
(Received 19 November 1979)

Reaction product of $MgCl_2$ with ethyl benzoate (EB) has a characteristic X-ray diffraction pattern. Plotted against the molar ratio of EB to $MgCl_2$, crystalline particle size of $MgCl_2$ shows a minimum while that of the reaction product was found independent on the molar ratio. Crystalline particle size of $MgCl_2$ in itself, and as a component of the EB/$MgCl_2$ support system, decreased rapidly in the course of grinding but reached practically constant values after a short period. Diffuse small-angle X-ray scattering of both supports and Ziegler–Natta catalysts on their basis was not changed by grinding the support.

INTRODUCTION

A considerable number of papers have been published about the highly active supported catalysts for polymerization of α-olefins in the past few years. Effects of mechanical[1-5] or chemical[3,6] activations of supports on the polymerization properties of the catalyst were studied. Crystal structure of the support[7,8] and ion radius of the metal component[9] in comparison with that of Ti^{4+} were related to the polymerization properties of the catalyst.

This paper is concerned with a further extension of knowledge about the supports by X-ray diffractometric investigations of the reaction between $MgCl_2$ and ethyl benzoate [EB], and of structural changes during mechanical grinding of $MgCl_2$ and EB/$MgCl_2$ systems.

EXPERIMENTAL

Preparation of $MgCl_2$ and EB/$MgCl_2$ samples

Anhydrous $MgCl_2$ was reacted with EB in different molar ratios under inert atmosphere (dried argon).

$MgCl_2$ and an EB/$MgCl_2$ system at molar ratio of 0.17 was ground in a vibration ball mill (1400 vibrations min^{-1}) for 0–120 h under inert atmosphere. Capacity of the ball mill was 0.5 dm^3 filled with 79 pieces of 11 diameter balls.

X-ray diffractometry

Wide angle X-ray diffractometric measurements were carried out by a Philips Müller Micro instrument in 2θ range of 4–55° at a recording rate of 0.5 deg min^{-1}.

The sample holder lid was equipped with a window of poly(ethylene terephthalate) (Mylar) film of 6.25 μm in thickness. Samples were filled in under inert atmosphere.

Recorded diffractograms were used for identification of samples and determination of crystalline particle size. The latter was calculated from the band width of the corresponding interference peak by the Laue–Scherrer equation:

$$D_{hkl} = \frac{\lambda K}{\beta \cos\theta}$$

$$\beta = \sqrt{\beta^2_{\mathrm{m}} - \beta^2_{\mathrm{inst}}}$$

where D_{hkl} — crystal size in direction perpendicular to the hkl plane (nm); λ — wave length of X-ray applied (Cu_K = 0.15418 nm); β — band width (radian); β_m — measured band width (radian); β_{inst} — instrument width (5×10^{-3} radian); θ — Bragg's angle; K — constant depending on the direction and on the shape of crystallites (for comparative measurements like the present ones, it can be regarded as 1).

It should be noted that particle sizes calculated by this equation involve a considerable uncertainty when β_m is only slightly higher than β_{inst}.

Small angle X-ray diffractometry was performed by a Rigaku–Denki equipment in 'step-scanning' regime from 0–40 min at a step-scanning of 100 s for each 0.5 min of 2θ. Samples were filled into Lindemann capillaries under inert atmosphere.

Experimental results were processed by two calculation methods:

(1) Guinier-plot (*Figure* 1) was used for determination of radius of gyration for inhomogeneities in the sample[10];

(2) Average diameter and diameter-distribution of the diameter of inhomogeneities were obtained by profile analysis of scattering curves.

Calculations for both methods were carried out by a Hewlett–Packard 9830 computer.

0032-3861/80/091037-04$02.00

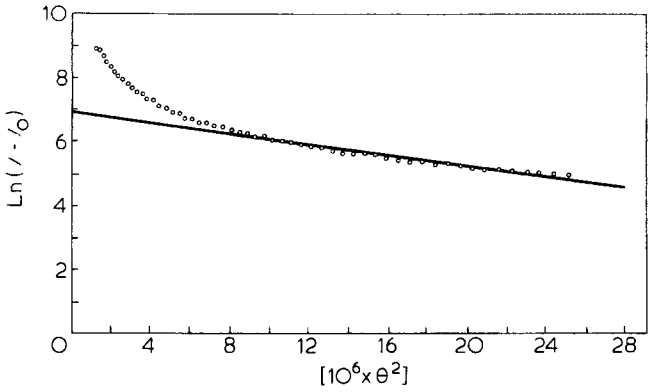

Figure 1 Guinier-plot of diffuse small angle X-ray scattering of $EB/MgCl_2/TiCl_4$ system at molar ratio of 0.17:1:0.05

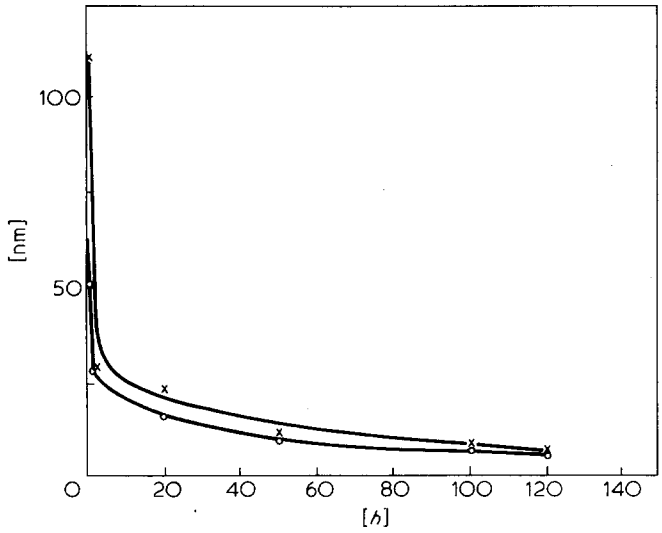

Figure 2 Changes in the crystalline particle size of $MgCl_2$ as a function of grinding time. $x = D_{001}$, $o = D_{110}$

RESULTS AND DISCUSSION

Changes in the crystalline particle size of $MgCl_2$ during grinding

The structure of anhydrous $MgCl_2$, though wellknown from the literature[11], is worth describing briefly in order to facilitate the interpretation of effects of grinding and interacting with EB on the structure of $MgCl_2$.

Crystalline $MgCl_2$ forms a hexagonal layer lattice. Within the layers, ionic bonds dominate but the covalent nature is also relevant. The individual layers can be considered as electrically compensated molecules linked to each other by secondary van der Waals forces.

X-ray diffractogram of anhydrous $MgCl_2$ is not rich in reflections which is favourable for the identification, on the basis of literary data[12]. The agreement was good.

Crystal sizes of unground $MgCl_2$ in directions perpendicular to the [001] and [110] planes are different, namely, 111 and 65 nm, respectively. Studying the changes in crystalline particle sizes during grinding, the above difference was found to disappear after a short grinding period simultaneously with a marked reduction in the overall crystalline particle size (*Figure* 2). Further grinding caused relatively small lessening in the particle size but its extent was nearly identical in both directions.

According to grinding theories[13], disintegrations occur primarily on deficient sites destroying the weakened bonds. In these regions, local stress maxima are generated during grinding which leads to fracture when the lattice strength is surpassed. In $MgCl_2$, defective sites are located within the layers while the weak bonds exist between the layers. For destruction of these secondary forces, less energy is needed than for disruption of ionic or covalent bonds within the layers. It is reasonable, therefore, that crystalline particle size of $MgCl_2$ decreases to a greater extent in the direction perpendicular to the [001] plane than to the [110] one.

The relatively little disintegration during further grinding beyond 1 h can be explained by the reduced amount of defective sites, and by the association of particles of high specific surface area. All these effects reach a dynamic equilibrium when particle size cannot be reduced by grinding.

X-Ray diffractometry of the reaction products from $MgCl_2$ and EB

Structural changes in $MgCl_2$ caused by EB were studied by wide-angle X-ray diffractometry at different molar ratios of EB to $MgCl_2$. In *Figure* 3, diffractograms of $EB/MgCl_2$ systems (at molar ratios of 0.10; 0.17; 0.25; 1.00 and 2.00) are compared with that of the pure $MgCl_2$. It can be seen that, besides the original reflexions, new bands appeared with increasing intensities as the amount of the ester was enhanced.

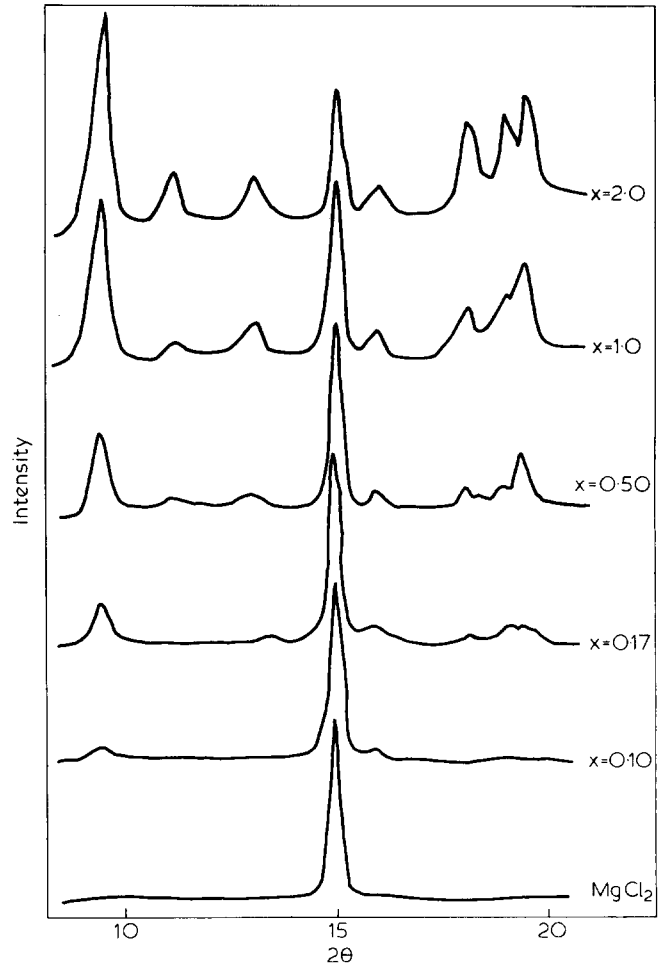

Figure 3 X-ray diffraction patterns of $EB/MgCl_2$ systems of different compositions (indicated are the molar ratios of EB to $MgCl_2$)

Table 1 2θ angles of the reflexion maxima of $MgCl_2$ and its reaction product with EB

$MgCl_2$	$EB/MgCl_2 = 2$
2θ values (deg)	
	6.6
	9.5
	11.2
	13.4
15.0	
	16.1
	18.1
	19.0
	19.6
	22.1
	24.2
	26.5
	29.8
30.4	
	32.4
35.2	
	36.6
	37.6
	38.4
	39.9
46.3	41.1
50.4	
50.6	

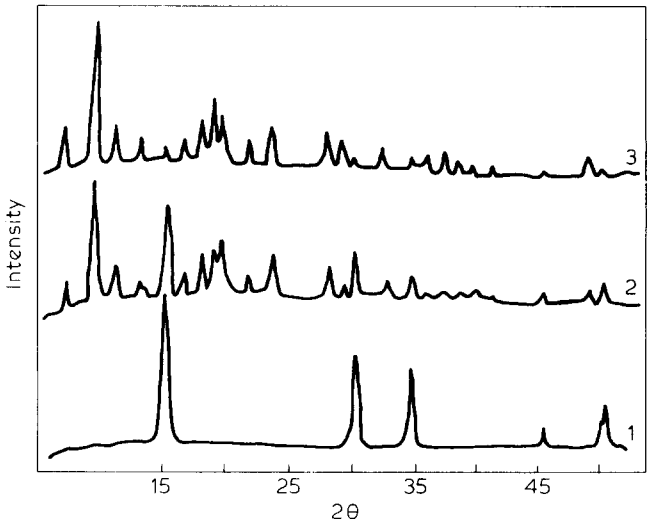

Figure 4 X-ray diffraction patterns of $MgCl_2$ (curve 1), $EB/MgCl_2 = 2$ system after 1 day (curve 2), and after 14 days (curve 3)

The new interference bands are not correspondent to any hydrated modifications of $MgCl_2$ [14], thus, they are not related to the strong hygroscopic nature of $MgCl_2$. Consequently, during the reaction between $MgCl_2$ and EB, a new crystalline material is formed with a characteristic interference pattern (*Table* 1). Crystalline particle size of this new species was determined by the half-width of the highest intensive band ($2\theta = 9.6°$, $d = 0.93329$ nm) being 23 to 25 nm, practically independent on the molar ratio. X-ray diffractograms of $EB/MgCl_2$ systems recorded on the 14th day after preparation were identical with those of fresh samples except for the molar ratio of 2.00. In the latter case, reflexions characteristic of $MgCl_2$ decreased to an insignificant level during 14 days (*Figure* 4). It demonstrates that an appropriate excess of the ester results in a complete destruction of the crystal structure of $MgCl_2$ in a longer reaction period.

Particle size of unreacted $MgCl_2$ in the $EB/MgCl_2$ systems as plotted against the molar ratio of EB to $MgCl_2$ shows a minimum at 0.17 (*Figure* 5). Further increase in the proportion of EB enhances the crystalline particle size even above its original level observed for pure $MgCl_2$.

It should be noted that this particular composition (molar ratio of EB to $MgCl_2 = 0.17$ or $MgCl_2$ to $EB = 6.0$) represents the support of most favourable polymerization properties.

Changes in the crystalline particle size during grinding of $MgCl_2$ with EB

Crystalline particle sizes of the unreacted $MgCl_2$ were determined in directions perpendicular to [001] and [110] planes at a molar ratio of EB to $MgCl_2$ of 0.17. As indicated above, crystalline particle sizes of $MgCl_2$ in the unground $EB/MgCl_2$ system were considerably smaller than those of the original $MgCl_2$ (*Table* 2).

It can be seen in *Table* 2 that D_{001} is much higher than D_{110} for $MgCl_2$ while in $EB/MgCl_2$ system D_{001} is somewhat lower than D_{110}. Thus, the reaction between $MgCl_2$ and EB diminishes the crystalline particle size of $MgCl_2$ even without grinding, especially in the direction perpendicular to the [001] layer lattice similarly to the effect of grinding.

Crystalline particle size of the $EB/MgCl_2$ system is markedly decreased by grinding for 20 h. Further grinding caused minor reduction in the particle size (*Figure* 6) indicating the attainment of a dynamic equilibrium as was demonstrated for the pure $MgCl_2$.

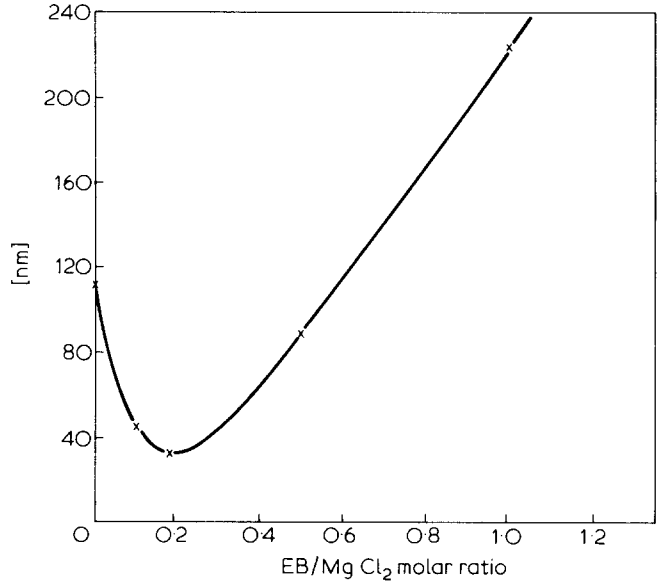

Figure 5 Changes in the crystalline particle size of $MgCl_2/D_{001}/$ as a function of the molar ratio of EB to $MgCl_2$

Table 2 Crystalline particle sizes of $MgCl_2$ in the original state and in the $EB/MgCl_2$ system at a molar ratio of 0.17 in directions perpendicular to [001] and [110] planes before grinding

Sample	D_{001} (nm)	D_{110}
$MgCl_2$ unground	111	65
$EB/MgCl_2 = 0.17$ unground	30.5	38

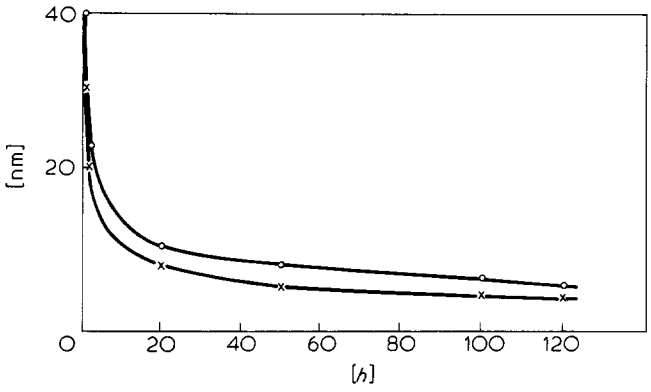

Figure 6 Decrease in the crystalline particle sizes of $MgCl_2$ in the EB/$MgCl_2$ = 0.17 system as a function of grinding time. $x = D_{001}$, $o = D_{110}$

Table 3 Small-angle X-ray diffractometric results for various support and catalyst preparations

Sample	Radius of scattering mass (nm)	Diameter of inhomogeneities (nm)
$MgCl_2$	5.8	6.9
$MgCl_2$ ground for 120^h	7.4	5.6
EB/$MgCl_2$ = 0.17 ground for 120^h	6.0	6.2
$MgCl_2/TiCl_4$ = 21*	6.6	7.1
EB/$MgCl_2/TiCl_4$* = 0.17:1:0.05	6.0	7.3

* The support was ground for 120^h

Small-angle X-ray diffractometry of the supports and supported catalysts

Diffuse small angle X-ray scattering[15] is proportional to the electron density differences of inhomogeneities in the material specifying the shape, size, and arrangement of electron density inhomogeneities. From changes in the diffuse X-ray scattering caused by mechanical and/or chemical treatments, conclusions can be drawn to the effects of electron density inhomogeneities of the support on the activity and stereospecificity of the catalyst prepared thereof.

$MgCl_2$ and EB/$MgCl_2$ systems (at molar ratio of 0.17) as supports and those treated with $TiCl_4$ as catalysts were studied. It can be seen in *Table* 3 that size and distribution of inhomogeneities in $MgCl_2$ (*Figure* 7) remained unchanged both by mechanical and chemical treatments. It can be concluded that the physical and chemical changes osberved in the present systems take place only on the surface of the support but these processes (such as disintegration, surface complex formation) are responsible for the polymerization properties of the catalyst.

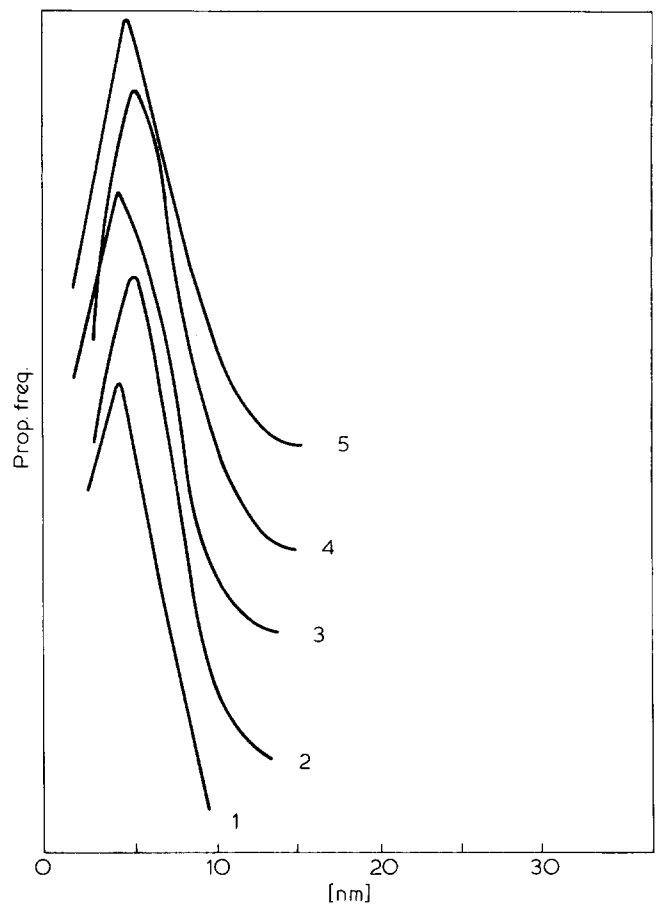

Figure 7 Diameter–distribution curves of small angle X-ray scattering. 1, $MgCl_2$; 2, $MgCl_2$ ground for 120 h; 3, EB/$MgCl_2$ = 0.17 ground for 120 h; 4, $MgCl_2/TiCl_4$ = 21 using $MgCl_2$ ground for 120 h; 5, EB/$MgCl_2/TiCl_4$ = 0.17:1:0.05 using EB/$MgCl_2$ ground for 120 h

REFERENCES

1 Arai, Y., Yasue, T. and Miyke, H. *J. Chem. Soc.* Japan 1972, **3**, 547
2 Rodriguez, L. A., von Looy, H. M. and Gabant, J. A. *J. Polym. Sci.* 1966, **4**, 1905, 1927, 1917, 1971
3 Ger. Off. 2 230 672
4 Ger. Off. 2 656 055
5 Br. Pat. 2 000 585
6 Ger. Off. 2 035 945
7 Keii, T. 'International Symposium on Macromolecular Chemistry', IUPAC, 1978, Tashkent
8 Haward, R. N., Roper, A. N. and Fletcher, K. L. *Polymer* 1973, **14**, 365
9 Soga, K., Katano, S., Akimoto, Y. and Kagiya, T. *Polymer J.* 1973, **5**, 128
10 Guinier, A. *Compt. rend. seances Acad. Sci.* 1927, **204**, 1115
11 Nåray-Szabó, I. 'Crystallochemistry', 1965, Akadèmiai Kiadò, Budapest
12 Standard: ASTM-D 25-1156
13 Hüttig, G. F. 'Neue Beobachtungen bei Zehrmahlungsvorgaengen und deren Deutung, 1952, Dechema Monographien
14 Standards: ASTM-D 1-947, 3-765, 1-1210, 25-515
15 Hoseman, R. and Bagchi, S. N. 'Direct Analysis of Diffraction by Matter', 1962, North Holland Publishing Co., Amsterdam